

34. H. W. Tipper, *ibid.*, p. 113; D. G. Taylor *et al.*, *ibid.*, p. 121.
35. A few terranes, such as the Cache Creek terrane, have extensive "Tethyan" coralline and fusulinid faunas that they may indeed represent far-traveled blocks; however, in consideration of the IWP affinities of the Galápagos hermatypic coral genera, the Cache Creek paleogeography may be difficult to resolve with fossil evidence alone.
36. P. Ziegler, *Geol. Rundsch.* **71**, 747 (1982).
37. N. F. Sohl, *J. Paleontol.* **61**, 1085 (1987).
38. By Cretaceous time, a tropical marine corridor connected the Atlantic and Pacific oceans; hence, the Cretaceous circumequatorial taxa may have dispersed westward using the Tethys current or possibly eastward using countercurrents or undercurrents; B. P. Luyendyk, D. Forsyth, J. D. Phillips, *Geol. Soc. Am. Bull.* **83**, 2649 (1972); E. G. Kauffman, *Geol. Assoc. Can. Spec. Pap.* **13**, 163 (1975).
39. G. Piccoli, S. Sartori, A. Franchino, *Mem. Sci. Geol. Univ. Padua* **38**, 207 (1986).
40. J. P. Kennett, *Marine Geology* (Prentice-Hall, Englewood Cliffs, NJ, 1982).
41. E. A. Kay, *Venus* **25**, 94 (1967); *Univ. Hawaii Harold L. Lyon Arboretum Lect.* **9** (1979), p. 1; *Bernice P. Bishop Mus. Spec. Publ.* **72**, 15 (1984).
42. H. A. Rehder, *Smithson. Contrib. Zool.* **289** (1980).
43. W. K. Emerson, *Venus* **25**, 85 (1967); *Nautilus* **92**, 91 (1978); *ibid.* **97**, 119 (1983).
44. P. W. Glynn and G. M. Wellington, *Corals and Coral Reefs of the Galápagos Islands* (Univ. of California Press, Berkeley, 1983); J. W. Wells, in *ibid.*, Appendix.
45. J. S. Garth, *Proceeding of the Second International Coral Reef Symposium* (Great Barrier Reef Committee, Brisbane, Australia, 1974), vol. 1, pp. 397-404; J. L. Barnard, *Smithson. Contrib. Zool.* **271** (1979); J. E. McCosker and R. H. Rosenblatt, in *Key Environments Galápagos*, R. Perry, Ed. (Pergamon, Oxford, 1984), pp. 133-144; R. C. Brusca, *Bull. Mar. Sci.* **41**, 268 (1987).
46. T. F. Dana, *Mar. Biol.* **33**, 355 (1975); R. W. Grigg, *Pac. Sci.* **35**, 15 (1981); R. W. Grigg, J. W. Wells, C. Wallace, *ibid.*, p. 1 (1981).
47. W. J. Zinsmeister and W. K. Emerson, *Veliger* **22**, 32 (1979).
48. R. S. Scheltema, *Biol. Bull.* **174**, 145 (1988).
49. K. L. Heck, Jr., and E. D. McCoy, *Mar. Biol.* **48**, 349 (1978).
50. P. L. Jokiel, *Coral Reefs* **3**, 69 (1984); J. Frazier *et al.*, *P. S. Z. N. I. Mar. Ecol.* **6**, 127 (1985).
51. R. S. Scheltema and I. P. Williams, *Bull. Mar. Sci.* **33**, 545 (1983); R. S. Scheltema, *ibid.* **39**, 241 (1986).
52. G. Thorson, *Biol. Rev. Cambridge Philos. Soc.* **25**, 1 (1950); S. A. Mileikovsky, *Mar. Biol.* **10**, 193 (1971); this is only a general estimate.
53. D. Jablonski and R. A. Lutz, in *Skeletal Growth of Aquatic Organisms*, D. C. Rhoads and R. A. Lutz, Eds. (Plenum, New York, 1980), pp. 323-377; D. Jablonski, *Bull. Mar. Sci.* **39**, 565 (1986), and many references therein.
54. J. A. Knauss, *Introduction to Physical Oceanography* (Prentice-Hall, Englewood Cliffs, NJ, 1978).
55. H. Pak and J. R. V. Zaneveld, *J. Geophys. Res.* **78**, 7845 (1973).
56. R. S. Scheltema, *Nature* **217**, 1159 (1968).
57. E. A. Kay and S. R. Palumbi, *Trends Ecol. Evol.* **2**, 183 (1987).
58. S. J. Nelson and E. R. Nelson, *Can. J. Earth Sci.* **22**, 442 (1985).
59. A. Gazdzicki and P. Reid, *Acta Geol. Polonica* **33**, 99 (1983).
60. G. D. Stanley, Jr., *U.S. Geol. Surv. Prof. Pap.* **1435**, 23 (1986); B. Senobari-Daryan and G. D. Stanley, Jr., *J. Paleontol.* **62**, 219 (1988); G. D. Stanley, Jr., and M. T. Whalen, in preparation.
61. D. L. Jones, N. J. Silberling, P. J. Coney, G. Plafker, *U.S. Geol. Surv. Map MF-1874A* (1987); J. W. H. Monger and H. C. Berg, *U.S. Geol. Surv. Map MF-1874B* (1987); N. J. Silberling, D. L. Jones, M. C. Blake, Jr., D. G. Howell, *U.S. Geol. Surv. Map MF-1874C* (1987).
62. A. M. Ziegler, C. R. Scotese, C. F. Barrett, in *Tidal Friction and the Earth's Rotation, II*, P. Brosche and J. Suendermann, Eds. (Springer-Verlag, New York, 1982), pp. 240-252.
63. I thank W. K. Emerson for his assistance with literature on eastern Pacific Mollusca.

# Energy Loss Mechanisms of Superconductors Used in Alternating-Current Power Transmission Systems

E. B. FORSYTH

**The intrinsic hysteretic loss of superconductors carrying alternating current has been derived from simple models and verified experimentally. In practical cable designs the losses are increased by surface roughness, conductor configuration, and added metallic components. When possible applications by electric utility companies are being considered, such losses are only one of many factors that must be adjusted in an optimization that produces the lowest cost (including both capital and operating expenses) during the lifetime of the system.**

THE DISCOVERY OF SUPERCONDUCTING MATERIALS WITH critical temperatures above 90 K (1) has rekindled interest in the practical application of superconductors. Will their high critical temperatures reduce refrigeration power or permit the use of nitrogen coolant, and are these important considerations in future applications? It is not clear if this is the case; such practical considerations depend on detailed analyses of prospective designs in which many factors are varied to optimize the overall system

performance. It is possible that the new superconductors will find applications at temperatures below half the critical temperature, where enhanced current-carrying ability may be an attractive feature. In commercial applications of superconductivity the capital cost must be balanced against other considerations that affect the operating costs. These considerations include maintenance, the projected load (over the lifetime of the project), and the expected losses; in a superconducting system the losses are manifested as the power needed to run the cooling system. The objective is usually to minimize the total cost over the lifetime of the system. Optimizations of this kind are typical of conventional engineering practice (2). For example, overhead transmission lines can easily be designed to lower resistive losses if bigger conductors are used, but this feature must be balanced against the cost of the larger conductor, stronger towers, and bigger insulators. In a superconducting power transmission system the conductor losses are a component, but not necessarily the major component, in setting the power level of the cooling system.

During the past three decades numerous projects were initiated in

The author is at Brookhaven National Laboratory, Associated Universities, Inc., Upton, NY 11973.

the United States, Europe, and the U.S.S.R. to develop superconducting transmission systems (3). A wide range of conductor configurations, conductor materials, and other design options were investigated. The largest project was at Brookhaven National Laboratory (BNL), where an outdoor test facility was used to evaluate flexible superconducting cables with a rating of 330 megavolt-amperes (MVA) per phase (1000 MVA on a three-phase basis). The site, which was operated for 4 years, provided a wealth of information on cable conductor losses. Many practical compromises had to be made in the cable design, some of which increased the losses above the intrinsic loss of the superconductor. An important consideration in selecting the material used in the conductor, niobium-tin ( $\text{Nb}_3\text{Sn}$ ), was the relatively high critical temperature of this material (about 18 K), which would allow useful savings in the refrigeration system (4). Another factor was the very high critical current density that permits cryostable operation with the very large fault currents that occur occasionally on all transmission networks; this characteristic improved the transient thermal performance and also reduced the conductor losses during normal operation. Unfortunately, most of the other solutions to the various technical problems involved in the design of the cable system resulted in increased losses. For example, the manufacture of the superconductor required very smooth surfaces to avoid loss enhancement. The addition of other components to strengthen the conductor increased the losses, and the helical configuration of the cable also resulted in higher losses. The mechanisms are described below.

Studies carried out with electric utility companies illustrated that losses are one characteristic of a complicated system that must be balanced against the cost of money (5, 6). The major losses in a superconducting power transmission system, which form the load for the refrigerator, arise from three sources: (i) current-dependent losses of the conductor, (ii) voltage-dependent losses of the insulation, and (iii) heat leakage of the cryogenic enclosure containing the cables. In addition, pumping losses must also be considered (7) when one is dealing with long, relatively narrow pipes.

## Conductor Losses

The magnitude of the current-dependent losses in superconducting cables carrying alternating current is the most imprecise component of the total losses. During the early phase of the development of superconducting power transmission cables, concern over conductor losses was a major factor in selecting a superconductor with a high first critical field ( $H_{c1}$ ) for this role, on the assumption that the Meissner effect assured zero hysteretic loss (8-10). Niobium (Nb) was first selected as a conductor for transmission cables but it has a low critical field and temperature compared to other type II superconductors. Bean has developed a theory of hysteretic loss in a type II superconductor (11). In his model he assumes a magnetic field,  $H_0$ , oriented parallel to the smooth surface of a superconductor at temperature  $T$ . The flux,  $B$ , inside the superconductor is zero at some depth as a result of a current flowing that locally is set by the critical current density  $J_c(H, T)$ . The magnetization,  $M$ , is defined as

$$4\pi M = B - H \quad (1)$$

and thus it is possible to calculate the area of the hysteresis loop when  $H_0$  is removed and restored. The loss of energy per unit volume per cycle,  $W$ , for a slab of superconductor can be expressed as

$$W = K H_0^3 / J_c \quad (2)$$

where  $K$  is a constant. This expression applies to a field magnitude

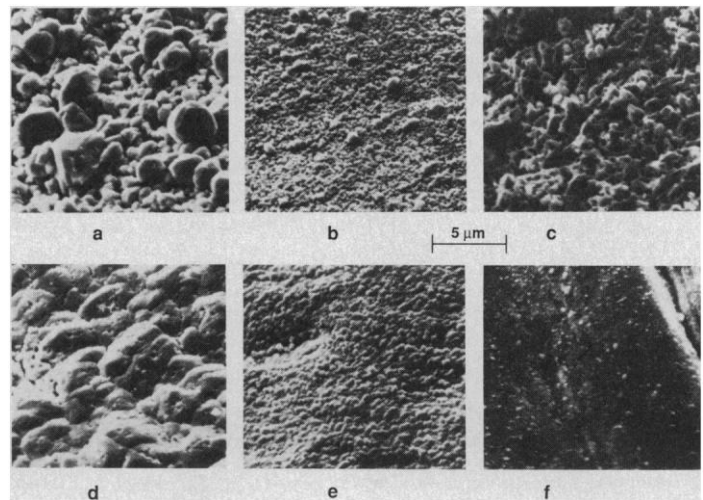


**Fig. 1.** Scanning electron micrograph of six  $\text{Nb}_3\text{Sn}$  superconductor samples that were evaluated at BNL in the 1970s: (a) IGC-1, (b) KB-15, (c) RCA-2119B, (d) CSCC-21, (e) BT-19, and (f) A-17. The surface roughness often depends on the method of preparation; for example, sample a is made by a liquid diffusion method and sample c is made by vapor deposition.

that is not large enough to eliminate the zero field region inside the superconductor. Bean has compared this diamagnetic phenomenon with the classic case of ferromagnetism in low magnetic fields (12).

As  $H_0$  increases, the zero-field region diminishes, and, when all the available conductor volume experiences a field, it is termed "saturated." In this case the losses do not increase as the cube of the field, because the volume of material exhibiting hysteretic loss is constant and the loss dependence with increasing field is predicted to ultimately approach a logarithmic function (13). When the analysis is extended to transport currents instead of an externally applied magnetic field, the loss is proportional to the square of the current for large currents (13). Hancox showed in 1966 that the losses were strongly dependent on the field component normal to the surface of the sample (13).

In very good samples the losses approached those predicted by the Bean model (14). However, at low fields, in the range zero to 400 A/cm [root mean square (rms)] at 4.2 K for  $\text{Nb}_3\text{Sn}$ , the losses are less than predicted by Bean. A phenomenological theory has been advanced by Fournet and Mailfert to explain the effect on the basis of the shielding of flux at the surface up to a certain level (15). During the course of research on the ac losses of superconducting materials, much of it conducted in the 1960s and early 1970s, it was found that the roughness of the surface, grain size, and sample purity exerted large effects on the losses. Once  $\text{Nb}_3\text{Sn}$  was prepared with a smooth surface (undulations typically less than 1  $\mu\text{m}$ ), its losses were lower than those of Nb, a result that was contrary to expectations at the time (16, 17), despite the fact that this result was predictable from the Bean model.

The losses discussed above can be considered intrinsic characteristics of a particular sample of superconductor (Figs. 1 and 2). Figure 1 shows the surface condition of six samples of  $\text{Nb}_3\text{Sn}$ . The losses for each sample are plotted as a function of surface magnetic field in Fig. 2. The correlation of surface roughness with loss has been discussed elsewhere (18). The losses of particular samples have been significantly reduced by chemical surface etching and even by mechanical polishing (19). The samples also demonstrate the flux shielding effect: the losses at low field are significantly below the predicted Bean loss. The losses of Nb were also dependent on the surface condition of the superconducting material; for example, electroplated Nb exhibited losses that were one-third to one-fourth, at the same field, of those of a welded conductor that had been cold-

worked (10).

Surface roughness may have an even more drastic effect on losses for the high-temperature ceramic superconductors because, so far, all samples are highly anisotropic. If a magnetic field normal to the surface induces a current along the  $c$  axis of the material, the greatly reduced  $J_c$  may result in very high losses if the Bean model applies.

Another important factor is the temperature dependence of the losses.  $J_c$  may be assumed to have a quadratic dependence on temperature,

$$J_c = J_0 [1 - (T/T_c)^2] \quad (3)$$

where  $J_0$  is the critical current density at absolute zero and  $T_c$  is the critical temperature. The losses have been calculated allowing for a temperature dependence of the surface exclusion field and are in agreement with experimental results (14). In general, the losses tend to rise quickly as the sample temperature approaches  $T_c$ , as a result of the reduction in  $J_c$ . This is an important consideration when one is choosing the mean temperature and temperature rise in an actual transmission system. Some insight into the behavior of loss magnitude as a function of temperature can be obtained by substituting for  $J_c$  in Eq. 2 the expression given in Eq. 3. At constant field magnitude,  $H_0$ , the power loss as a function of temperature,  $P(T)$ , is given by

$$P(T) = \text{constant}/[1 - (T/T_c)^2] \quad (4)$$

The power required at room temperature (300 K) is given by the Carnot relation

$$P(T)/P_{300} = K_2 [T/(300 - T)] \quad (5)$$

where  $K_2$  is known as the coefficient of performance (COP), usually expressed as a percentage of Carnot efficiency. COP varies markedly with the rating of the refrigerator (20), ranging from about 5% for a 1-W refrigerator to 22% for a 20-kW machine. Typical transmission line refrigerators will have a capacity of 20 to 100 kW with helium coolant. From previous experience of large installations, COP is above 20%; thus, about 205 W of input power will be required to maintain an isothermal load at 7 K dissipating 1 W. In practice, the load is not isothermal and the simple calculation of Eq. 5 must be modified (21). A machine producing liquid nitrogen at 77 K would require about 11 W per watt of load.

Equations 4 and 5 can be combined to show how the power at room temperature varies with  $T/T_c$ . Power is a minimum when  $T$  is approximately  $0.6 T_c$ . Above this minimum the advantage of a high  $T_c$  may be lost, and as  $T$  approaches  $T_c$  the system may not be cryostable, that is, a short heat pulse, possibly the result of a momentary current overload, may cause  $T$  to rise indefinitely.

If this criterion were applicable to the new superconductors, which have a  $T_c$  of approximately 90 K, it would imply that the maximum operating temperature would not exceed 54 K, too low to allow nitrogen to be considered as a coolant. However, the total heat load on the refrigerator also includes other sources, as mentioned above, and these may not have the same temperature dependence as the conductor losses. The choice of mean operating temperature and allowable temperature rise must be made as part of an optimization of the complete system design.

The temperature dependence of losses for small samples of  $Nb_3Sn$  is illustrated in Fig. 3. Because  $J_c$  appears in the denominator of Eq. 2, it is important to ensure that  $J_c$  at the operating temperature is as high as possible. A good fit to measured curves was obtained with  $J_c$  of  $\sim 6 \times 10^6$  A/cm<sup>2</sup> at 4.2 K, implying a value of  $J_0$  in Eq. 3 of  $\sim 6.4 \times 10^6$  A/cm<sup>2</sup>.

A generic conductor design consists of superconducting material attached to other metal layers. In the case of rigid conductors the metal layer is also the supporting pipe. Flexible conductors usually have normal metal attached to both surfaces. These components of the conductor are required for strength and to provide flux-jump stabilization: they usually increase the losses above the intrinsic loss of the superconductor alone. Rigid conductors made by plating or soldering superconductor to a supporting pipe are subject to various

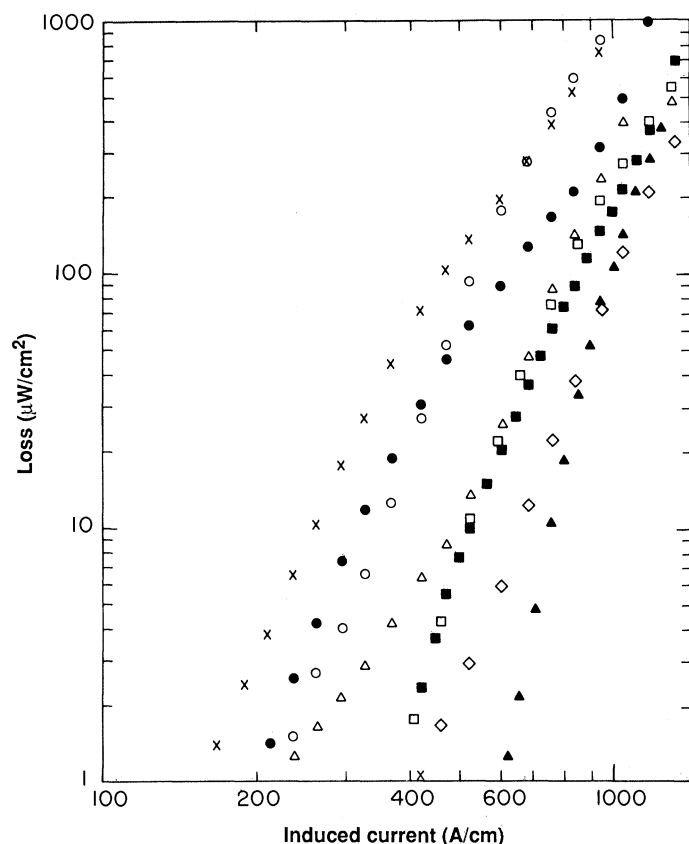


**Fig. 2.** Hysteretic loss at 60 Hz of five of the six samples shown in Fig. 1 (plus three additional samples): sample a in Fig. 1,  $\times$ ; sample b,  $\square$ ; sample d,  $\Delta$ ; sample e,  $\blacksquare$ ; sample f,  $\blacktriangle$ ; IGC-4,  $\circ$ ; IGC-6,  $\bullet$ ; and A-1,  $\diamond$ . The loss at 500 A/cm (current per unit width) varies by two orders of magnitude between samples. The lowest loss is associated with sample f in Fig. 1; the highest loss with sample a. The data strongly suggest a correlation between surface roughness and loss, which was confirmed in other experiments.

**Table 1.** Physical properties of the cable conductor. See also Fig. 7.

Measure	Value
Inner conductor diameter (over outer tape)	29.5 mm
Inner conductor tape width	6.5 mm
Number of superconducting tapes (two layers)	20
Outer conductor diameter (under inner tape)	52.7 mm
Outer conductor tape width	11.7 mm
Number of superconductor tapes (two layers)	20
Tape thickness	110 $\mu\text{m}$
Copper thickness	50 $\mu\text{m}$
Stainless steel thickness	30 $\mu\text{m}$
Thickness of $Nb_3Sn$ (each surface per tape)	$\sim 4$ $\mu\text{m}$
Specified loss at 500 A/cm and 4.2 K (with cladding)	$< 15$ $\mu\text{W}/\text{cm}^2$
Specified minimum bend radius of the tape	$< 1$ cm
Specified quench current at 4.2 K and 60 Hz (self field)	$> 2500$ A per centimeter of width
Transition temperature	$> 16.5$ K
Design temperature range	6.0 to 8.0 K

loss mechanisms; plated conductors exhibit loss dependence caused by surface conditions. Soldered conductors have exhibited losses caused by cracking on cooldown. Both types are usually designed in relatively short lengths prior to installation, of the order of 20 m. Thus numerous superconducting field joints are required, which will probably increase the current-dependent losses.

Flexible conductors made with corrugated sections also are subject to loss enhancement caused by surface deterioration during the corrugating process, but experimental data are sparse (22). In the case of flexible cables with twisted conductors, the pitch or twist of separate conductors produces both circumferential and axial components of magnetic field. These fields can, in turn, induce eddy currents in the normal metal cladding attached to the superconductor and even in the walls of the cryogenic envelope (23). The eddy currents flowing in normal metals can produce losses far in excess of the hysteretic loss of the superconductor.

Another loss mechanism associated with the metal cladding is due to the solder used in making the attachment. Lead-tin solder is a lossy superconductor below  $\sim 7$  K and should be avoided (24). Thin metal layers (known as a "flash") deposited to aid in the adhesion of solder can also increase the losses substantially. Nickel was used for this purpose in some early superconducting tapes, but it is ferromagnetic and a very thin layer causes noticeable losses (24).

The subject of ac losses in superconductors is complex (25), and the brief discussion above is intended only to demonstrate the scope of the problem. A summary of metallurgical and materials processing leading to the use of low-loss  $\text{Nb}_3\text{Sn}$  for ac transmission cables has been published (26).

## Losses in Helically Wound Conductors

All superconducting cable designs are of a coaxial configuration with full current capability in both inner and outer conductors. This feature reduces eddy currents in the envelope surrounding the cables. In the early design of a flexible cable at BNL it was proposed to wind the inner and outer conductors of the cable from helically wound tapes. The tapes form a cylindrical surface and are wound in the same left- or right-handed sense (27). A number of small trial samples were made with the single helical configuration for each conductor. The superconducting cable made by Siemens also was based on single helices with a Nb wire conductor (23). The disadvantage of a single helix is that a residual axial component of magnetic field is present. This field may increase the losses by inducing eddy currents in the vessel surrounding the cable (28) or in the supporting cable core. Experimental confirmation of this loss mechanism was obtained during the test of the Siemens cable (23). The most serious objection to the single helix conductor is not the added loss mechanism but the fact that the axial flux gives rise to a longitudinal voltage drop on the outer conductor of the cable (29). This drop would complicate grounding and generate undesirable effects during faults. A full discussion of the design of cable conductor must include consideration of contraction, fault current stabilization, ground currents, and economic implications (30). The numerous technical designs to satisfy these constraints have been discussed (31).

Two advantages are gained with the use of flexible cables: (i) the economic advantage achieved by installing long lengths from a reel, and (ii) the technical advantage of absorbing the contraction of the cable components when cooling down from room temperature to within a few degrees of absolute zero. These advantages can be retained and the axial magnetic field eliminated if each conductor (inner and outer) is wound with two helical layers, each laid in the opposite sense. The move to a double helix conductor is not an easy

choice as the configuration is clearly more complicated and expensive. In addition, new loss mechanisms are present in the double helix as compared to the single helix.

The general assembly of the BNL cable is shown in Fig. 4, and current flow in the two superconducting tapes forming the inner conductor is shown in Fig. 5. For the inner conductor the choice of a pitch angle of  $45^\circ$  results in two currents that are nearly equal in magnitude in the two layers. The current flow is not the same in each layer, however (32). The current flows in a corkscrew pattern in the outermost layer and parallel to the tape edges in the innermost layer (Fig. 5). The net result is that the axial magnetic field is zero in the annulus between the inner and outer conductors, and the current flow on the upper surface of the outermost tape, which is parallel to the conductor axis, produces only a circumferential magnetic field. The conductor configuration causes extra loss mechanisms owing to two effects: (i) current flows in three surfaces, and (ii) current crosses from one surface to another on the same tape, giving rise to a loss associated with the properties of the substrate of the tape.

The increase in loss in the  $\text{Nb}_3\text{Sn}$  caused by the first effect is larger by approximately a factor of 2 than that for a single tape conductor. The surface magnetic field between the two layers is approximately 70% of the field in the annulus between the inner and outer conductor. The losses in the substrate depend on whether the material is superconducting. The subject has been examined experimentally (33), and the properties of the substrate material have been varied to determine the effect on the losses (31).

Many of the effects described above were examined in detail during the testing of the prototype 1000 MVA system at BNL (34).

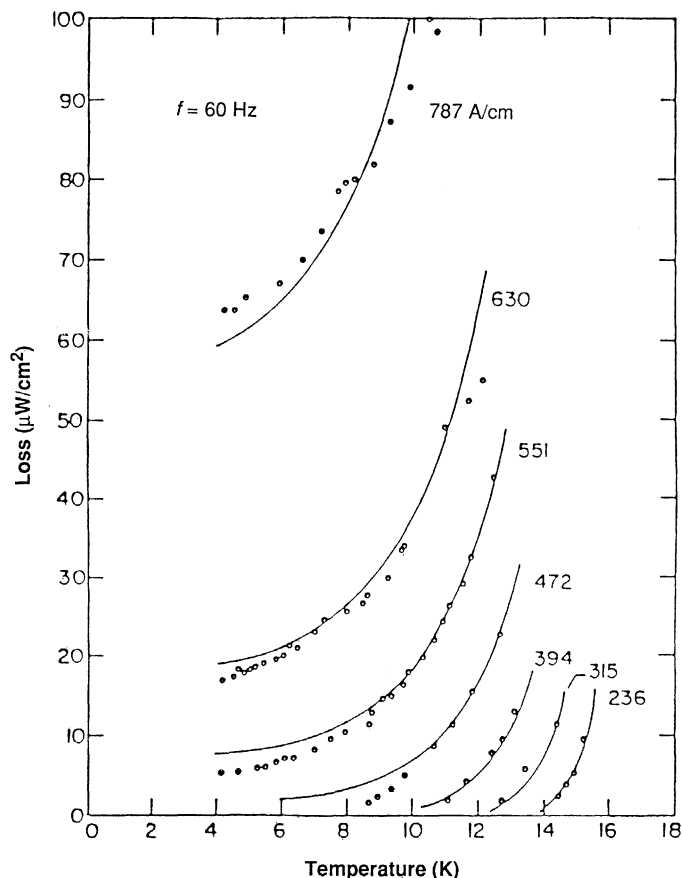
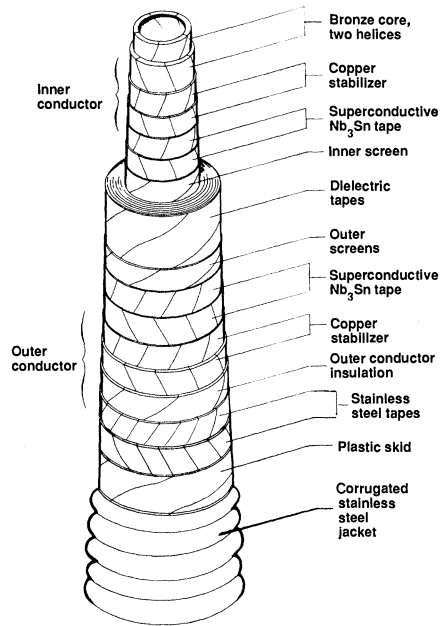


Fig. 3. The temperature dependence of hysteretic loss at 60 Hz for  $\text{Nb}_3\text{Sn}$  samples. The surface field (in amperes per centimeter) is shown for each set of points. The solid lines are theoretical fits based on the theory of Fournet and Mailfert (15). The data are from (14).

**Fig. 4.** General assembly of the flexible cable developed at BNL. A flexible bronze mandrel supports the four tapes that make up the inner conductor. The inner conductor is surrounded by the dielectric insulation (polypropylene tape). The outer conductor is a mirror image of the inner conductor with wider tapes. The corrugated jacket forms the pressure vessel for high-pressure helium coolant.



The test results also brought to light an additional loss mechanism. The losses of the inner and outer conductor of two cables, each 110 m in length, were measured over a wide range of current and temperature. The loss is expressed in watts per meter of cable for an excitation frequency of 60 Hz. The loss as a function of temperature is shown in Fig. 6. These data can only be understood with a knowledge of the detailed construction of the cable shown in Fig. 4. The cable consists of two current-carrying conductors separated by lapped polypropylene tape insulation. Each conductor consists of four metallic tapes: two copper (Cu) tapes and two superconducting tapes, each pair of tapes wound in the form of helices that twist in opposite directions. The construction of the cable has been described in detail (31, 35). The superconducting tapes consist of a laminated structure shown in cross section in Fig. 7. The Cu layer is the stabilizer, and stainless steel is added to strengthen the laminate and to keep the neutral axis near the superconducting layer; a strain greater than 0.1% can cause permanent degradation of the tape properties (31). The stainless steel and Cu layers experience the magnetic field present between the two superconducting tapes and should be chosen to minimize loss in these cladding layers (31). The superconducting component is formed of Nb<sub>3</sub>Sn on the two surfaces of a Nb substrate. Considerable processing is provided during fabrication to minimize losses before the cladding materials are laminated to the superconductor (36). The superconductor is made by running a Nb strip through molten Sn and then reacting to form the compound Nb<sub>3</sub>Sn. The resulting tape is ultimately slit to provide two tapes of different widths, used on the inner and outer conductors. Because the tape is slit, it does not have Nb<sub>3</sub>Sn covering the edges. Some physical properties and dimensions of the cable conductor and tape are given in Table 1. A comparison of conductor losses with the intrinsic loss of the superconductor is given in Table 2.

Several conclusions may be drawn from the data in Table 2. The loss enhancement of the inner conductor, >4.4, confirms earlier experiments (33, 37) and indicates the magnitude of the substrate loss; a loss of a factor of 4 to 5 is to be expected. The loss enhancement of the outer conductor, >7.2, reflects the fact that the losses of the outer conductor may be expected to decrease compared to the inner conductor by the ratio of the diameters of the conductors, 1.78. This did not occur, and the losses of each conductor are about the same. Taken in conjunction with the

measured exponent of the loss dependence, 2.0, the conclusion can be drawn that the conductor acts as if it were saturated. Because there is an adequate volume of superconductor available to carry the current, it is believed that the current is crowded to the edges of the tape, and the saturated conditions in that region cause the losses there to predominate. The square law dependence of losses as a function of current strongly suggests that the current is approaching the critical magnitude at the edges; such a dependence conforms with the analysis by Hancox (13). Thus the inner and outer conductor losses are approximately the same because both conductors have the same number of edges.

The existence of a proximity effect, which causes a variation of current density across a conductor carrying alternating current, has been known for many years (38), particularly for radio frequency applications; the effect was also considered for round superconducting wires (39) and flat tapes (40) in single-helix conductors. Loss enhancement factors were calculated by Ward *et al.* (40), assuming superconducting edges, a condition that is not met by the tapes used in the BNL cable. Nevertheless, enhancement by at least a factor of 2 was predicted because of the sharp corners. The paths of current flow shown in Fig. 5 are redrawn in Fig. 8 to show diagrammatically the effect of nonlinear current distribution in the tapes. The effect causes the current to flow in discrete "bands" parallel to the cable axis when one is viewing the outer tape of the inner conductor.

Grossly nonlinear current distribution is not the only explanation of the loss dependence on current. A simple resistive term would

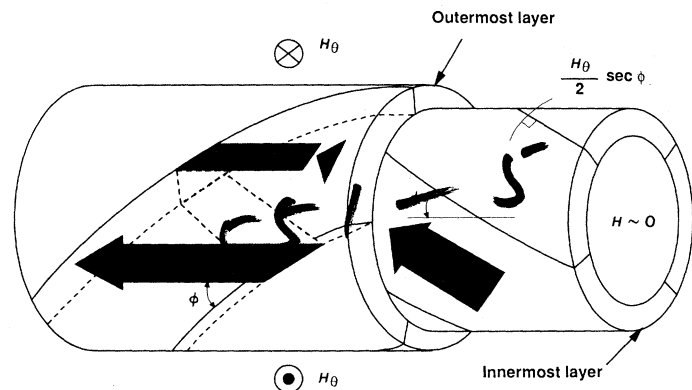


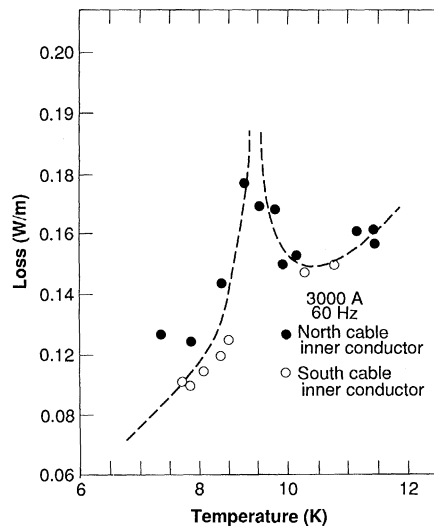
**Fig. 5.** Current flow in the two tapes forming the inner conductor of a cable (31); ⊙, vector coming out of the page; ⊗, vector going into the page. The double helix configuration eliminates the axial component of magnetic field at the expense of higher losses due to the fact that current flows on three surfaces and in the edges of the outermost tape.

**Table 2.** Comparison of conductor loss.

Measure	Value
Measured inner conductor loss at 441 A/cm, 7.7 K	190 mW/m
Measured outer conductor loss at 441 A/cm, 7.7 K	180 mW/m
Single tape loss (inner conductor) at 500 A/cm, 7.7 K	122 μW/cm <sup>2</sup>
Single tape loss (outer conductor) at 500 A/cm <sup>2</sup> , 7.7 K	115 μW/cm <sup>2</sup>
Specified tape loss at 500 A/cm, 4.2 K*	<15 μW/cm <sup>2</sup>
Specified tape loss at 500 A/cm, extrapolated to 7.7 K†	<28 μW/cm <sup>2</sup>
Loss enhancement in inner conductor tape	>4.4
Loss enhancement in outer conductor tape	>7.2
Ratio of inner diameter to outer diameter	1.78
Exponent of loss versus current	2.0

\*Includes an eddy current loss of ~5 W/cm<sup>2</sup> in the copper cladding. †Using curve in (14) for extrapolation.

**Fig. 6.** Inner conductor loss at 3000 A (60 Hz) as a function of temperature. The peak in the loss at approximately 9 K is caused by the current flowing in the Nb substrate of the tape. These losses peak at the critical temperature of Nb.



produce a quadratic dependence of loss with current. Such resistive loss could arise from very small zones of normal material in the tape, perhaps caused by microscopic cracks in the superconductor. Another resistive loss mechanism may be current flowing from tape to tape. These mechanisms were investigated during the laboratory tests of 10-m-long cables without definitive results (37). The loss dependence on temperature (Fig. 6) also argues against a simple resistive loss term. One loss measurement technique used at the 1000 MVA test site permits the loss waveform to be examined; this demonstrated the harmonic content characteristic of hysteretic loss. However, during the 4-year testing period the loss of the outer conductor of the north cable apparently increased by about 20 to 30 W. This loss may have been related to repairs carried out on a termination. This loss could be explained by an increase in the resistance of the outer conductor by a little over a microhm; the increase has caused the dissipation to roughly double at full current. The comparisons in Table 2 do not reflect the later, higher, value of outer conductor loss.

**Table 3.** Projected operating loss of the existing 1000 MVA prototype at BNL.

Measure	Value
Maximum thermally limited current	4100 A
Maximum conductor losses, three phases per kilometer at 7 K mean	1 kW
Maximum thermally limited power	1000 MVA
Service or normal daily power rating	670 MVA
Service current	2750 A
Conductor losses, three phases per kilometer at 670 MVA	450 W
Load factor	80%
Average load	540 MVA
Current at minimum load (410 MVA)	1680 A
Conductor loss, three phases per kilometer at 410 MVA	168 W
Average loss over 24 hours	310 W
Heat leakage of enclosure per kilometer	500 W
Voltage-dependent loss, three phases per kilometer	150 W
Total average loss, service load at 7 K, per kilometer	960 W
Total loss, thermal limit, at 7 K, per kilometer	1790 W
Service rating room-temperature input power to refrigerator,* per kilometer	216 kW
Transmission efficiency for 160 km, power loss per thermal rating (at service rating)	3.5%
Transmission efficiency for 160 km, continuous thermal rating	6.4%

\*Based on a system efficiency of 225 W/W.

The data on the dependence of loss on the cable temperature (Fig. 6) are subject to fairly large errors. For example, the system rarely reached thermal equilibrium, the temperatures at each end of the cable were not the same, and the temperature measurements are subject to error. Numerous other factors contributed to error in the measurements; for instance, small differences in the inner and outer conductor currents caused the instrumentation to erroneously show large apparent losses. The techniques of loss measurement with electronic and calorimetric methods have been described for relatively small samples (25). Loss measurements of long cables require that special probe wires be incorporated into the construction (41). Nevertheless, the system demonstrated the peak in losses centered on 9 K, which was also observed in laboratory tests on smaller cables (33, 37). This peak is caused by the high losses in the substrate that reach a peak at the critical temperature of Nb. This effect obscures that part of the loss produced by the current flowing in the Nb<sub>3</sub>Sn layers. Comparison with the temperature dependence of the intrinsic loss (14) suggests that loss enhancement caused by this effect may occur at temperatures as low as 7.5 K. Thus the enhancement factors shown in Table 2 probably reflect a component attributable to this effect. It would be desirable to eliminate the loss component caused by the substrate, but a method of making the conductor with superconducting edges and at the same time maintaining good quality control for long lengths of tape has not been found.

## Operational Factors

When a superconducting power transmission system is placed in operation, many losses will always be present; for example, heat leakage into the enclosure and voltage-dependent losses must be absorbed regardless of the power carried by the cables. If there is good control of the load power factor, the cable current is proportional to the power carried by the transmission system and thus the conductor losses vary by roughly the square of the power delivered. Superconducting transmission lines will always constitute major facilities, comparable to the existing 345-kV, 550-kV, and 765-kV overhead lines. Thus it may be assumed that the service operating conditions of the two methods are comparable. By and large, the system operators try to base-load major transmission facilities, that is, maintain a constant power level that is not greatly affected by the daily load cycle that characterizes the total power generated and consumed in a pool. This is very difficult to achieve in practice, and the load factor (ratio of average to maximum power transmitted) depends on the specifics of the distribution of generation and load within a pool or utility company. The load factor for a large transmission line is at least 80%. Thus the current-dependent losses in a superconducting transmission system with a similar load factor would vary by a factor of about 1.6 during daily operation. In order to obtain the total losses, it would be necessary to integrate over the day and the total would depend on the shape of the load curve.

Another operating condition also complicates the exact determination of conductor losses. All major transmission facilities must be designed to carry a continuous contingency power that is larger than the normal operating level. The margin between the maximum thermal rating and the normal operating level provides the reliability necessary to maintain total power flow in the event of a transmission line failure. In the case of a superconducting transmission system the maximum contingency rating depends on the capacity of the refrigeration system to absorb the increase in conductor losses above those associated with the normal daily operation. The economic impact of these losses is relatively small—the capital cost of the cooling system would increase slightly—but the cost of losses at the contingency level over a long period will be negligible because it

must be assumed that failures are relatively rare and the cost of losses will in most cases reflect normal daily operating conditions.

Table 3 shows the operating characteristics of the existing prototypical system at BNL. The conductor-dependent losses at the thermally limited rating of 1000 MVA is 1000 W/km. At the service rating of 670 MVA (two-thirds of the thermal rating) with 80% load factor, the losses fall to an average of 310 W/km, based on 12 hours at 670 MVA and 12 hours at 410 MVA. Addition of thermal losses of the enclosure and voltage-dependent losses produces a total heat load for the refrigerator of 960 W/km at the service or normal daily rating of 670 MVA with 80% duty factor. For a transmission line 160 km long, this would correspond to a total average loss of about 3.5% of the thermal rating. A more detailed extrapolation of this design to a double circuit installation, each circuit rated 1000 MVA thermally, has been published (42). It was pointed out in that study that the efficiency of superconducting transmission systems will be less for circuits with ratings in the 1000 MVA range than for systems with thermal ratings up to 5000 MVA, which is probably the highest that could be envisaged in the foreseeable future.

A study of the operational characteristics of a projected superconducting power transmission system raises a number of important questions:

1) What level of cable losses is technically and economically acceptable to the electric utility companies? This is another way of asking what should be the current density in the conductor and electric field in the cable insulation?

2) In what proportions should the three major sources of loss in a superconducting system be divided?

Unfortunately there are no precise or analytic solutions to these questions. Even in transmission systems designed on the basis of conventional engineering techniques, there are wide variations caused by specific site and route considerations. The first question was first asked over a hundred years ago when the lines connecting the first generators at Niagara Falls were being designed to carry power to Buffalo. Lord Kelvin suggested that the annual cost of

carrying charges should equal the annual cost of the losses (43), and this would result in an economical design. This philosophy still applies: in the first study of an electric utility system carried out by BNL workers near the start of the R&D project, it was proposed to use a shielded enclosure for the cables that had a very low leakage of heat into the refrigerated zone, but the cost was too high (5). Overall, it was less expensive to accept a higher heat leakage into the refrigerated zone and a lower capital cost, but the assumptions concerning the cost of energy and the cost of money must be valid over the entire projected life of the installed system, clearly an impossibility. Similar concerns affect the design of conventional underground transmission facilities (44).

The choices of current density and electric field for the cable design are made to satisfy a number of considerations. In the early work on the design of superconducting cables at BNL it was believed that the ability to design for surge impedance loading (SIL), when the cable impedance and load impedance are matched, was very important (45). In practice, designs that have thermal limits of 0.75 to 2 SIL will probably find application. The ratio of surface magnetic and electric fields in the cable is set by the condition that load and cable impedances are matched. In the BNL cables, the cables and load are matched for surface fields of 400 A/cm and 10 MV/m. Thus the losses at 400 A/cm must be acceptable, and the dielectric loss and 30-year reliability of the insulation must be acceptable for a 60-Hz stress of 10 MV/m.

The apportionment of losses depends on many considerations including the line rating, route length, and anticipated load factor during the service life. Economic analyses carried out during the project (5, 46) indicate that the following apportionment may lead to acceptable designs: current-dependent loss, 30%; voltage-dependent loss, 20%; and enclosure heat leakage, 50%. These percentages depend on the line rating and route. The most comprehensive study of overall methods of underground power transmission economics was carried out for the Department of Energy by the Philadelphia Electric Company (PEC) in 1976. The company evaluated 16 technical designs, including 3 with superconducting cables, all designed to carry a total of 10,000 MW over a distance of 105 km (6). This route, from the Susquehanna River to Philadelphia, was under consideration by the planning department as an anticipated need in the 1990s. Subsequent events in the world energy market and the scaled-back capital investment strategy of the electric utility companies have severely modified this plan, but the evaluation based on the use of many criteria accepted by the power companies was a useful exercise. The cost of losses of the BNL design, based on

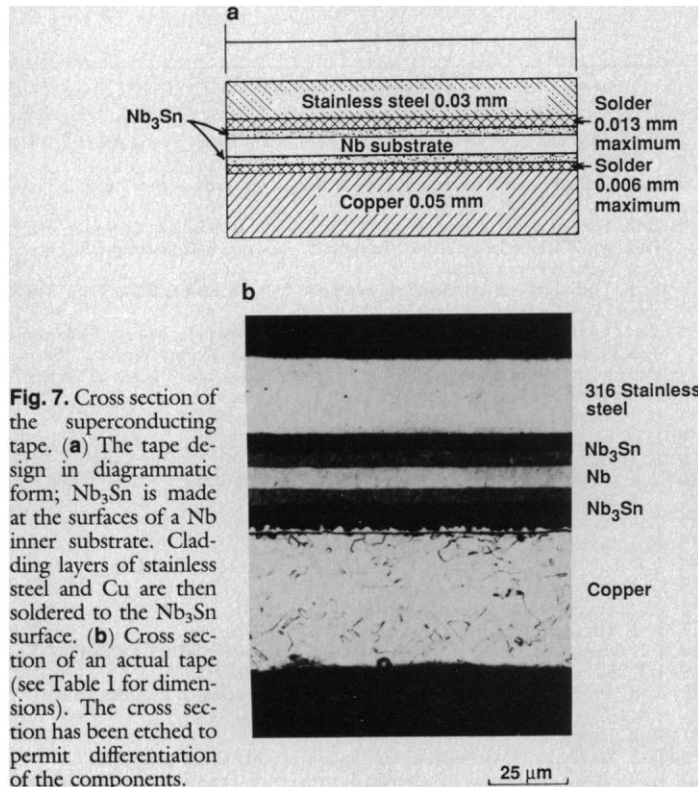


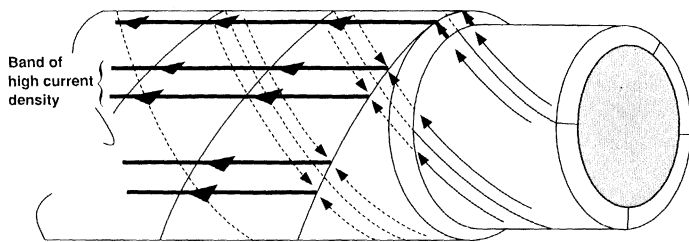
Fig. 7. Cross section of the superconducting tape. (a) The tape design in diagrammatic form; Nb<sub>3</sub>Sn is made at the surfaces of a Nb inner substrate. Cladding layers of stainless steel and Cu are then soldered to the Nb<sub>3</sub>Sn surface. (b) Cross section of an actual tape (see Table I for dimensions). The cross section has been etched to permit differentiation of the components.

Table 4. Cost of losses in the BNL design evaluated in the Philadelphia Electric Company Study (6).

Measure	Value
Cable losses	70 MW
Cable loss per year	611 × 10 <sup>3</sup> MW-hour
Capitalized cable loss cost*	\$66 million
Demand cost† of cable loss	\$32 million
Transformer losses	63 MW
Transformer losses per year	395 × 10 <sup>3</sup> MW-hour
Capitalized transformer loss cost	\$43 million
Demand cost† of transformer loss	\$29 million
Compensation loss	0.2 MW
Compensation loss per year	955 MW-hour
Capitalized compensation loss cost	\$100,000
Demand cost† of compensation loss	\$75,000
Total capitalized losses	\$170 million
Total installation cost	\$1,295 million
Capitalized loss as percentage of total	13%

\*A 40-year life at 16.3% carrying charge.

†Cost of generation to supply loss.



**Fig. 8.** It can be inferred from the loss data that the current density is nonlinear because of proximity effects. The pattern shown in Fig. 5 is modified here to indicate this effect. Current on the outside surface of the inner conductor is concentrated in bands; the number of bands equals the number of tapes used to construct one layer of the conductor. The current does not cross the gap between the tapes; it circulates underneath to emerge on top of the next band.

flexible cables as evaluated by the PEC, is shown in Table 4. Three circuits were proposed, each with three cables, at a thermal rating of 5000 MW per circuit. It should be noted that the accounting methods used to determine these costs are arcane and beyond the scope of this article.

The energy loss attributable to compensation and transformation have been included in Table 4. Compared to overhead lines, superconducting cables will carry the same amount of power at much lower voltage, probably reduced by a factor of 4, and thus considerable voltage transformation will be required to properly integrate a superconducting system into an existing network so that the correct division of load flow is achieved. Compensation is required to maintain voltage levels and system stability during faults. Proper SIL should eliminate the need for extra reactive compensation, but in practice a wide range between the normal daily rating and maximum thermal rating (which may well be typical of superconducting systems) may always require some reactive compensation, possibly switched in and out, depending on network conditions. The losses of the reactive compensation can be substantial if the correct matching impedances are not achieved. The BNL design did not suffer from high compensation system losses. On a capitalized basis with a 40-year life, the total cost of the losses was 13% of the total estimated cost of the system. This should be compared with the life cycle cost of losses of other technical designs. For example, three high-pressure, oil-filled cable designs had losses of 21 to 23%, which included a substantial contribution from shunt compensation reactors. A rigid superconducting system had losses of 9%, but the estimated total life cycle cost was twice that of the flexible superconducting cable system. The losses of a dc superconducting system represented 18% of the total life cycle cost, in part because of the conversion losses of ac to dc and dc to ac. The study indicated that superconducting systems could be economically competitive with other technologies, but overall losses did not play a decisive role in considerations of the relative merits of the various options.

## Conclusions

The current-dependent losses of superconducting material in alternating fields can be predicted from theory only for well-prepared samples in fields parallel to the surface. In practical conductors the losses can be substantially increased by surface roughness, large grain size, and the addition of other materials to the superconductor. Further increases in loss occur in practical cable configurations as a result of nonuniform current distribution. The BNL cables also exhibit a loss peak at a temperature that depends on the material used in the tape substrate; this characteristic was accepted as a compromise between losses and conductor cost. At

present there is no analytical model that convincingly explains the loss characteristics observed in the cables at the 1000 MVA test site.

In actual service in an electrical utility network, the losses will be set by the load factor and daily load cycle. These can never be predicted precisely in advance, and designers will strive to balance many factors to achieve an acceptable optimized system. These factors include total losses, capital cost, reliability, stability margins, and load flows under normal daily and contingency conditions. It is simplistic to believe that superconducting transmission systems will be operated with low losses unless energy costs rise dramatically in the future; studies of several technologies including superconducting systems have resulted in estimates for the life cycle cost of losses, all of which lie within a narrow range. Superconducting power transmission systems will be capable of carrying very large amounts of power for long distances. If these features can be achieved at competitive costs, it seems likely that the utility companies will turn to this technology should the installation of conventional overhead lines be proscribed for environmental or aesthetic reasons or because of lack of space near load centers.

Despite the many compromises that had to be made in the conductor design, the BNL prototype demonstrated that a large system meeting the predicted technical characteristics could be built and operated with losses that would be economically acceptable to utility companies. It seems likely that the test results obtained with the prototype will lead to ways of reducing the losses. A reduction by a factor of 2 is desirable; further reductions would give designers the option of designing cables carrying three to four times the SIL. Since the work at BNL on Nb<sub>3</sub>Sn tape in the mid-1970s, it has become possible to obtain multifilamentary composites with Nb<sub>3</sub>Sn filaments less than 2 μm in diameter (47). These conductors are certainly worthy of evaluation for the next generation of cable designs. If the new ceramic materials can be developed to provide the same critical current densities (of the order of 3 × 10<sup>6</sup> to 6 × 10<sup>6</sup> A/cm<sup>2</sup>) in appropriate conductor configurations, it would be desirable to measure the losses and proceed with design studies to determine the optimum operating temperature and other technical characteristics of the system.

## REFERENCES AND NOTES

1. M. K. Wu *et al.*, *Phys. Rev. Lett.* **58**, 908 (1987).
2. E. D. Eich and S. P. Walldorf, *IEEE Trans. Power Appar. Syst.* **PAS-102**, 3348 (1983); H. D. Short, *ibid.*, p. 3355.
3. E. B. Forsyth, in *Encyclopedia of Physical Science and Technology* (Academic Press, Orlando, FL, 1987), vol. 13, p. 465.
4. E. B. Forsyth *et al.*, in *Proceedings of the Applied Superconductivity Conference* (IEEE Publ. no. 72CH0682-5 TABSC, Institute of Electrical and Electronic Engineers, New York, 1972), p. 202.
5. E. B. Forsyth, G. A. Mulligan, J. W. Beck, J. A. Williams, *IEEE Trans. Power Appar. Syst.* **PAS-94**, 161 (1975).
6. *The Evaluation of the Economical and Technological Viability of Various Underground Transmission Systems for Long Feeds to Urban Areas* (report prepared for the Department of Energy by the Philadelphia Electric Company, National Technical Information Service Publ. no. NCP/T-2055/1, Springfield, VA, 1977).
7. G. H. Morgan and J. E. Jensen, *Cryogenics* **17**, 257 (1977).
8. P. A. Klaudy, *Adv. Cryog. Eng.* **11**, 684 (1965).
9. R. W. Meyerhoff, *Cryogenics* **11**, 91 (1971).
10. ——— and W. T. Beall, Jr., *J. Appl. Phys.* **42**, 147 (1971).
11. C. P. Bean, *Rev. Mod. Phys.* **36**, 31 (1964).
12. Lord Rayleigh, *Philos. Mag.* **5**, 23 (1887).
13. R. Hancox, *Proc. IEE (London)* **113**, 1221 (1966).
14. J. F. Bussiere, M. Garber, S. Shen, *Appl. Phys. Lett.* **25**, 756 (1974).
15. G. Fournet and A. Maiffert, *J. Phys. (Paris)* **31**, 357 (1970).
16. M. Suenaga and M. Garber, *Science* **183**, 952 (1974).
17. R. E. Howard *et al.*, *Adv. Cryog. Eng.* **22**, 332 (1976).
18. J. F. Bussiere, M. Garber, M. Suenaga, *IEEE Trans. Magn.* **MAG-11**, 324 (1975).
19. J. F. Bussiere and M. Suenaga, *J. Appl. Phys.* **47**, 707 (1976).
20. T. R. Strobridge, *Report EPRI 282* (Electric Power Research Institute, Palo Alto, CA, 1975).
21. R. B. Jacobs, *Adv. Cryog. Eng.* **7**, 567 (1961).
22. P. A. Klaudy and J. Gerhold, *IEEE Trans. Magn.* **MAG-19**, 656 (1983).
23. G. Bogner, P. Pencznski, F. Schmidt, *Siemens Forsch. Entwicklungsber.* **8**, 1 (1979).

24. J. F. Bussiere, M. Garber, M. Suenaga, *J. Appl. Phys.* **45**, 4611 (1974).
25. V. Kovachev, *Energy Dissipation in Superconducting Materials* (Oxford Univ. Press, Oxford, in press).
26. J. F. Bussiere, *IEEE Trans. Magn.* **MAG-13**, 131 (1977).
27. E. B. Forsyth *et al.*, *IEEE Trans. Power Appar. Syst.* **PAS-92**, 494 (1973).
28. J. Sutton, *Cryogenics* **15**, 541 (1975).
29. G. H. Morgan and E. B. Forsyth, *Adv. Cryog. Eng.* **22**, 434 (1976).
30. J. Sutton and D. A. Ward, *Cryogenics* **17**, 495 (1977).
31. J. F. Bussiere, V. Kovachev, C. Klamut, M. Suenaga, *Adv. Cryog. Eng.* **24**, 449 (1978).
32. M. Garber, J. F. Bussiere, G. H. Morgan, in *Conference on Magnetism and Magnetic Material 1976* (AIP Conference Proceedings no. 34, American Institute of Physics, New York, 1977), p. 84.
33. M. Garber, *IEEE Trans. Magn.* **MAG-15**, 155 (1979).
34. E. B. Forsyth and R. A. Thomas, *Cryogenics* **26**, 599 (1986).
35. E. B. Forsyth, in *Proceedings ICEC9* (Ilfic, Guildford, England, 1982), p. 202.
36. P. H. Brisbin, P. S. Swartz, K. W. Pickard, *IEEE Trans. Magn.* **MAG-15**, 146 (1979).
37. G. H. Morgan, F. Schauer, R. A. Thomas, *ibid.* **MAG-17**, 157 (1981).
38. S. Butterworth, *Proc. R. Soc. London Ser. A* **107**, 693 (1925).
39. D. A. Ward and R. J. Bray, *Cryogenics* **15**, 21 (1975).
40. D. A. Ward, B. J. Maddock, W. S. Kytce, *ibid.* **19**, 339 (1979).
41. F. Schauer, *A Theory of Losses and Loss Measurements of Superconducting Power Cables Consisting of Helically Wound Conductor Tapes* (Informal Rep. BNL 15644, Brookhaven National Laboratory, Upton, NY, 1982).
42. E. B. Forsyth and R. A. Thomas, *IEEE Trans. Power Delivery* **PWRD-1**, 10 (1986).
43. Lord Kelvin, *Br. Assoc. Rep.* (1881), p. 526.
44. *Report EL-5279* (Electric Power Research Institute, Palo Alto, CA, 1987).
45. E. B. Forsyth, in *International Conference on High Voltage and/or ac Power Transmission* (Institute of Electrical Engineering, London, 1973), p. 40.
46. ———, J. R. Stewart, J. A. Williams, in *1976 Underground Transmission and Distribution Conference* (IEEE Conference Record no. 76 CH1119-7-PWR, Institute of Electrical and Electronic Engineers, New York, 1976), p. 446.
47. A. K. Ghosh, K. E. Robins, W. B. Sampson, *IEEE Trans. Magn.* **MAG-21**, 328 (1985).
48. Brookhaven National Laboratory is operated by Associated Universities, Inc., under a contract to the U.S. Department of Energy. The work at Brookhaven mentioned in this article is supported by the Department of Energy. I acknowledge many useful discussions of the physics underlying loss mechanisms in superconductors with M. Garber and G. H. Morgan. R. A. Thomas assisted in the analysis of data obtained at the 1000 MVA test site and in the extrapolation to future designs. The effect of unbalanced conductor currents on loss measurement was analyzed by M. Meth in *Correction of Cable Loss Measurement Due to Current Unbalance* [BNL Tech. Note PTP 137 (Brookhaven National Laboratory, Upton, NY, 1983), unpublished].

# Phenotypic Diversity Mediated by the Maize Transposable Elements *Ac* and *Spm*

SUSAN R. WESSLER

Mutations caused by the insertion of members of the *Ac* or *Spm* family of transposable elements result in a great diversity of phenotypes. With the cloning of the mutant genes and the characterization of their products, the mechanisms underlying phenotypic diversity are being deciphered. These mechanisms include (i) imprecise excision of transposable elements, which can result in the addition of amino acids to proteins; (ii) DNA methylation, which has been correlated with the activity of the element; (iii) transposase-mediated deletions within elements, which can inactivate an element or lead to a new unstable phenotype; and (iv) removal of transcribed elements from RNA, which can facilitate gene expression despite the insertion of elements into exons. An understanding of the behavior of the maize elements has provided clues to the function of cryptic elements in all maize genomes.

MAIZE TRANSPOSABLE ELEMENTS ARE RESPONSIBLE FOR a remarkable variety of unstable mutant phenotypes. The phenotypes of several alleles, each containing the transposable element *Ds*, for example, can differ in (i) the frequency, timing, and quality of somatic mutations caused by excision of *Ds* from the gene during plant development and (ii) the residual level of gene expression observed in the absence of *Ds* excision. Plant

geneticists had characterized these distinctive patterns of somatic mutation before recombinant DNA techniques were available. The accuracy of these early studies is a tribute to the geneticists and to their choice of experimental organism.

This review focuses on well-characterized examples of phenotypic diversity generated by transposable elements in maize. Remarks are largely confined to mutations caused by the *Ac* and *Spm* (or *En*) families of maize transposable elements. For a more detailed discussion of plant transposable elements, the reader is referred to several excellent reviews on the genetics and molecular biology of transposable elements in maize in particular (1, 2) and plants in general (3, 4).

The maize plant is an ideal genetic system for studying the phenotypic subtleties displayed by controlling element alleles. Sensitive genetic markers are available for observing the insertion and excision of the elements in virtually all organs. Notable among these are seven loci (*a*, *a2*, *c*, *c2*, *bz*, *bz2*, and *R*) involved in the biosynthesis and deposition of anthocyanin pigments in different organs of the maize plant. Mutation of any one of these loci eliminates or alters the wild-type purple color in some or all tissues. In addition to the anthocyanin loci, genes involved in the production of endosperm starch [that is, *shrunkened* (*sh*) or *waxy* (*wx*)], when mutated, can alter the morphology of the kernel or the quality of the starch. These also are easily scored markers that have been important in the study of the genetics and molecular biology of maize.

## Nomenclature

The maize transposable elements studied by McClintock were called controlling elements to emphasize their ability to regulate the

The author is assistant professor in the Botany Department, University of Georgia, Athens, GA 30602.